Title
Autoregulation of Neurogenesis by GDF11

Journal
Neuron, 37(2)

ISSN
0896-6273

Authors
Wu, Hsiao-Huei
Ivkovic, Sanja
Murray, Richard C
et al.

Publication Date
2003

DOI
10.1016/s0896-6273(02)01172-8

Neuron, Vol. 37, 197–207, January 23, 2003, Copyright ©2003 by Cell Press

Autoregulation of Neurogenesis by GDF11

Hsiao-Huei Wu,[1] Sanja Ivkovic,[2] Richard C. Murray,[1] Sylvia Jaramillo,[1] Karen M. Lyons,[2] Jane E. Johnson,[3] and Anne L. Calof[1,*]

[1]Department of Anatomy and Neurobiology and The Developmental Biology Center
University of California, Irvine
Irvine, California 92697

[2]Department of Molecular, Cell, and Developmental Biology
University of California, Los Angeles
Los Angeles, California 90095

[3]Center for Basic Neuroscience
University of Texas Southwestern Medical Center
Dallas, Texas 75390

Summary

In the olfactory epithelium (OE), generation of new neurons by neuronal progenitors is inhibited by a signal from neurons themselves. Here we provide evidence that this feedback inhibitory signal is growth and differentiation factor 11 (GDF11). Both GDF11 and its receptors are expressed by OE neurons and progenitors, and GDF11 inhibits OE neurogenesis in vitro by inducing $p27^{Kip1}$ and reversible cell cycle arrest in progenitors. Mice lacking functional GDF11 have more progenitors and neurons in the OE, whereas mice lacking follistatin, a GDF11 antagonist, show dramatically decreased neurogenesis. This negative autoregulatory action of GDF11 is strikingly like that of its homolog, GDF8/myostatin, in skeletal muscle, suggesting that similar strategies establish and maintain proper cell number during neural and muscular development.

Introduction

The sizes of neuronal populations are critical determinants of nervous system function and are under tight genetic control (Williams, 2000). In the vertebrate nervous system, the gradual slowing and then cessation of progenitor cell proliferation toward the end of embryonic development (Caviness et al., 1995; Kauffman, 1968) suggests that neurogenesis is under some form of negative control. Experiments on model systems support the idea that differentiated neurons produce signals that feed back to inhibit the generation of new neurons by neuronal progenitors (Mumm et al., 1996), but the molecules that mediate such effects in vivo have not been identified. Elucidating such negative growth signals is likely to be very important, not only for understanding nervous system development, but also for devising strategies to deal with brain injury and aging, in which persistent growth-inhibitory signals could thwart attempts to promote regeneration.

To understand the molecular regulation of neurogenesis, we study a model neuroepithelial tissue, the olfactory epithelium (OE) of the mouse. The OE is morphologically and functionally similar to the neuroepithelia that generate the nervous system, but has significant advantages as a system for study. The OE is simpler, producing only one major type of neuron, the olfactory receptor neuron (ORN). Significantly, the OE retains both its epithelial morphology and the ability to generate neurons throughout life (Calof et al., 1996a). In addition, application of a variety of experimental approaches has allowed identification of different cell stages in the ORN lineage and revealed important features of the regulation of neurogenesis in this system. Among these is the finding that neuron production in the OE is governed by negative signals, which play at least as important a role as positive signals in this system (Calof et al., 2002).

In the OE, tight regulation of neurogenesis serves to maintain the size of its neuronal population at a particular level. Thus, in normal animals in which ORNs are constantly dying in low numbers (due to disease or injury), a low level of neurogenesis is constantly replacing them. If experimental manipulations are used to induce death of large numbers of ORNs, the production of new neurons (by proliferation of neuronal progenitors that reside within the basal layers of the epithelium) is rapidly upregulated until the original state of the OE is restored (reviewed in Calof et al., 1996a). An in vitro correlate of this phenomenon is the observation that proliferation and generation of new ORNs by cultured OE neuronal progenitors is inhibited by the presence of large numbers of differentiated ORNs (Mumm et al., 1996). Such experiments have provided strong support for the idea that ORNs produce a signal that feeds back to inhibit production of new neurons by their own progenitors.

Because of their known actions in inhibiting cell growth, as well as neural induction, we have focused on signaling molecules of the transforming growth factor-β (TGF-β) superfamily as candidates for feedback inhibitors of neurogenesis (Shou et al., 1999, 2000). Here we provide in vitro and in vivo evidence that a recently identified member of this superfamily, growth and differentiation factor 11 (GDF11), acts as such a feedback inhibitory signal in the OE. Thus, one way in which the mammalian nervous system achieves proper neuron number during development is by negative autoregulation of neurogenesis. In the OE, GDF11 and its antagonist, follistatin, are critical regulators of this process.

Results

Expression of *Gdf11* and Its Putative Receptors by Neurons and Neuronal Progenitors

The TGF-β superfamily, a large group of secreted proteins with widespread roles in development and tissue homeostasis, can be divided into two groups on the basis of similarities in structure and downstream signaling pathways: the TGF-β/activin group and the Dpp/bone morphogenetic protein (BMP) group (Newfeld et al., 1999). GDF11, a recently identified member of a

*Correspondence: alcalof@uci.edu

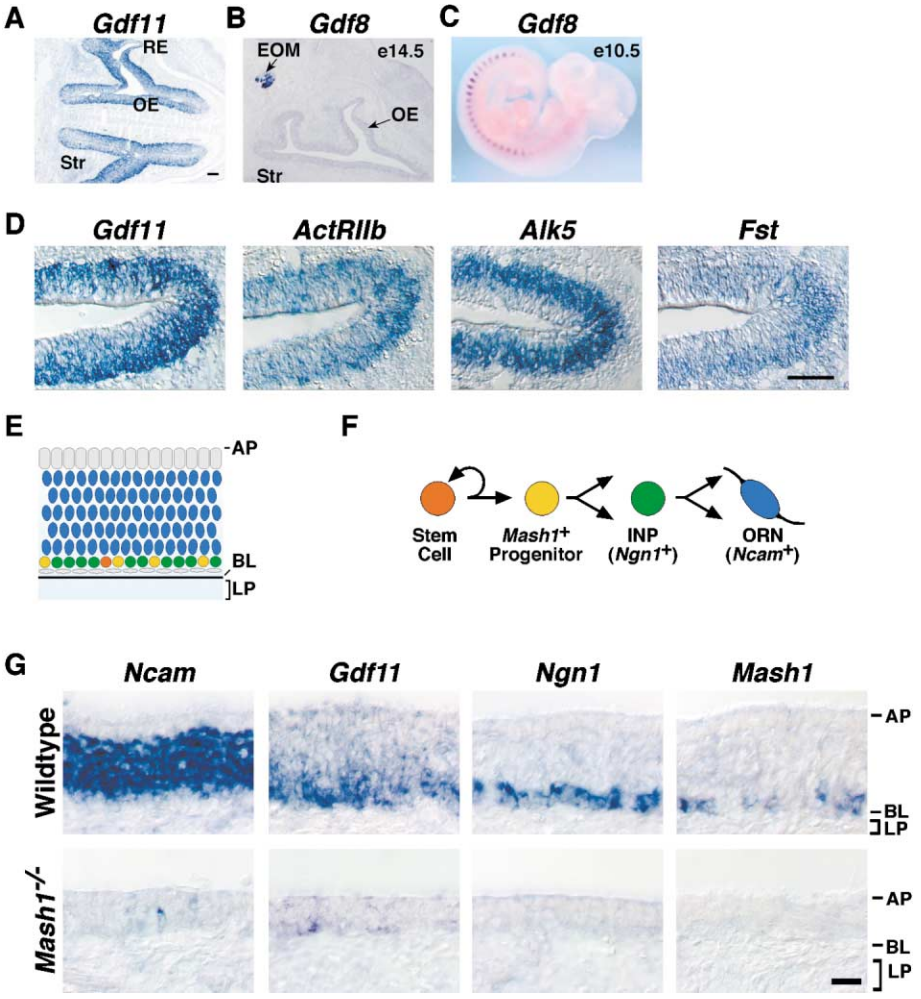

Figure 1. *Gdf11* and Components of the GDF11 Signaling Pathway Are Expressed in E14.5 Olfactory Epithelium

(A) *Gdf11* is expressed specifically in olfactory (sensory) epithelium. OE, olfactory epithelium; RE, respiratory epithelium; Str, stroma. Bar, 100 μm.

(B) *Gdf8* is not expressed in OE. EOM, extraocular muscle.

(C) *Gdf8* is expressed in developing somites in E10.5 mouse embryos.

(D) *Alk5*, *ActRIIb*, and *Fst* are expressed in a pattern similar to that of *Gdf11* in OE at E14.5. Bar, 100 μm.

(E) Diagram of laminar arrangement of cells in the OE. Sustentacular cells, gray; ORNs, dark blue; INPs, green; MASH1$^+$ progenitors, yellow; stem cells, orange; horizontal basal cells, gray.

(F) Neuronal lineage of the OE (Calof et al., 1998, 2002).

(G) *Gdf11* is expressed by ORNs and their progenitors. OE from E17.5 *Mash1*$^{-/-}$ embryos and wild-type littermate was hybridized with probes to *Ncam*, *Gdf11*, *Ngn1*, and *Mash1*. Bar, 20 μm. AP, apical surface; BL, basal lamina; LP, lamina propria.

small subfamily of the TGF-β/activin group, came to our attention after a report showing its expression in the epithelium lining the nasal cavity (Nakashima et al., 1999). GDF11 is 90% identical in amino acid sequence to GDF8/myostatin, a factor that is expressed by muscle cells, inhibits proliferation of myoblasts in culture, and when absent causes mice to exhibit increased skeletal muscle mass (Lee and McPherron, 1999; McPherron et al., 1997; Taylor et al., 2001; Thomas et al., 2000). Because this is the same type of action we envisioned for feedback inhibition of neurogenesis, we performed in situ hybridization experiments to determine if *Gdf11* and components of its signaling pathway have appropriate patterns of expression in the OE (Figure 1).

In mouse OE, *Gdf11* expression is first evident at embryonic day 12.5 (E12.5), and continues to be expressed through adulthood (data not shown). At E14.5—the age at which the neuronal lineage is fully established and there is a high level of neurogenesis in the OE (Calof and Chikaraishi, 1989)—we found *Gdf11* expression in the nasal mucosa to be confined to the olfactory (sensory) epithelium, with no expression in adjacent respiratory epithelium (Figure 1A). *Gdf11* expression in facial and neural tissues near the OE appeared to be confined to the eye (lens and neural retina): no expression was evident in OE stroma; in facial mesenchyme surrounding the OE; or in the olfactory bulbs, with which developing ORNs make synaptic contact (data not shown; see Nakashima et al., 1999). The *Gdf11* homolog *Gdf8*, in contrast, is not expressed in OE, but as expected is present

in developing head and trunk muscle (Figures 1B and 1C). At higher resolution, *Gdf11* expression was seen to be confined to the basal two-thirds of the OE, the region that contains ORNs and their progenitors (Figure 1D). A similar expression pattern was observed for *ActRIIb* and the type I TGF-β receptor *Alk5*, which other work has suggested are the likely ligand binding and signaling receptors for GDF11 (Figure 1D) (Federman et al., 2000; Lee and McPherron, 2001; McPherron et al., 1999). Interestingly, *follistatin* (*Fst*), a secreted antagonist of GDF11 (Gamer et al., 1999), is also expressed in OE, as well as its underlying stroma (Figure 1D).

Within OE proper reside both neuronal cells (ORNs and their progenitors) and two nonneuronal cell types, sustentacular cells (supporting cells found in a single, apical layer) and horizontal basal cells (keratin-expressing cells that lie immediately atop the basal lamina) (Figure 1E). The neuronal cells of the OE, which occupy the intervening layers, consist of ORNs and the three progenitor cell types of this neuronal lineage (Figure 1F). Thus, there are four distinct stages in the ORN lineage (reviewed in Calof et al., 2002): (1) a self-renewing stem cell, which gives rise to (2) neuronal progenitors that express the bHLH transcription factor MASH1. MASH1-expressing progenitors give rise to (3) immediate neuronal precursors (INPs), which express the bHLH transcription factor, Neurogenin1 (Ngn1). INPs divide to give rise to daughter cells that undergo terminal differentiation into (4) ORNs. Differentiated ORNs extend axon processes to the olfactory bulb of the brain, where they form synapses and express differentiation markers such as the neural cell adhesion molecule, NCAM.

To determine which OE cell types express *Gdf11*, we took advantage of *Mash1*$^{-/-}$ mice. Genetic studies have shown that *Mash1* function is required for generation of ORNs (Guillemot et al., 1993). In *Mash1*$^{-/-}$ mice the ORN lineage is cut short at an early stage, as *Mash1*-expressing neuronal progenitors initially form, but then undergo apoptosis (Calof et al., 1996b; Cau et al., 1997; Murray et al., in press). Thus, the OE of *Mash1*$^{-/-}$ mice is markedly thinner than that of wild-types, and expression of *Ngn1* and *Ncam* is drastically reduced since the epithelium lacks most ORNs and ORN progenitors (Figure 1G). When we examined the OE of *Mash1*$^{-/-}$ embryos, we found that *Gdf11* expression was essentially absent (Figure 1G). Since sustentacular cells and horizontal basal cells are still present in *Mash1*$^{-/-}$ mice (Guillemot et al., 1993; Murray et al., in press), this indicates that the cells that express *Gdf11* must be ORNs and ORN progenitors.

GDF11 Inhibits Development of the Progenitor Cells that Give Rise to Olfactory Receptor Neurons

An early indication that GDF11 was likely to exert a negative effect on OE neurogenesis came from pilot studies with GDF8 (which appears to activate the same signaling pathways as GDF11 [Federman et al., 2000; Lee and McPherron, 1999, 2001; McPherron et al., 1999; Oh and Li, 1997] and was initially more readily available). In these studies, we assessed effects of GDF8 on neuronal colony formation in vitro, an assay that gives a sensitive and quantitative overall picture of OE neurogenesis, but does not reveal the cellular stages at which effects occur (Mumm et al., 1996; Shou et al., 1999, 2000). We observed that GDF8 (10 ng/ml) treatment caused a 95% ± 5% decrease in the number of neuronal colonies that developed in these assays, compared to untreated controls.

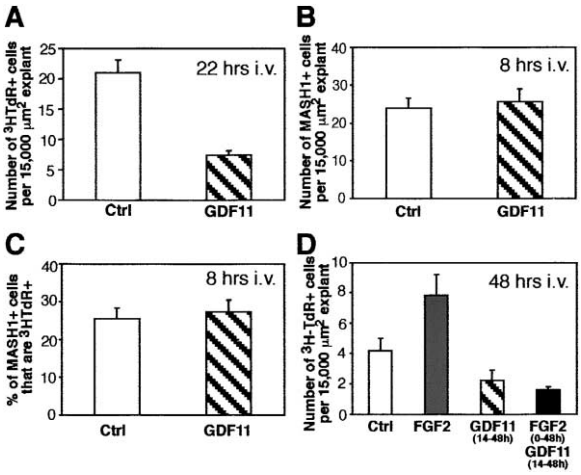

Figure 2. GDF11 Inhibits OE Neurogenesis In Vitro

(A) Fewer neuronal progenitors are present in GDF11-treated cultures. OE explants were cultured for 22 hr with GDF11 (20 ng/ml) or no added factor, and ^{3}H-TdR$^+$ cells surrounding each explant counted. $p < 0.05$, Student's t test.

(B) GDF11 does not affect MASH1$^+$ progenitor cell number. Explants were cultured with or without GDF11 (20 ng/ml) for 8 hr and MASH1 immunoreactive cells surrounding each explant counted.

(C) GDF11 does not affect proliferation of MASH1$^+$ progenitors. Explants were cultured 8 hr, with ^{3}H-TdR added for the final 2 hr. The percentage of MASH1$^+$ cells that were also ^{3}H-TdR$^+$ was determined.

(D) GDF11 prevents FGF-stimulated proliferation of INPs. OE explants were treated with FGF2 (10 ng/ml), GDF11 (20 ng/ml), or both as indicated. ^{3}H-TdR was added for the final 24 hr in vitro, and ^{3}H-TdR$^+$ cells surrounding each explant counted. $p < 0.05$, Dunnett test. Error bars, SEM for (A)–(D).

With this information in hand, we turned to testing GDF11 itself, and to using assays that provide more detailed information about cellular targets of growth factor action, such as short-term OE explant cultures in which individual cells are easily identified and counted. Initially, OE explants were cultured for 22 hr in GDF11, with ^{3}H-thymidine (^{3}H-TdR) added for the last 6 hr to mark neuronal progenitors in S phase. As shown in Figure 2A, GDF11 caused a large decrease in the number of progenitors incorporating ^{3}H-TdR, compared with untreated cultures. This indicates that GDF11 indeed has negative action on OE neurogenesis, and acts to inhibit proliferation of OE neuronal progenitor cells.

We have shown previously that a different TGF-β superfamily ligand, BMP4, has an antineurogenic action in the OE neuronal lineage that is exerted on MASH1-expressing neuronal progenitors. BMP4 binding to these cells targets preexisting MASH1 protein for rapid degradation via the proteasome pathway, resulting in cessation of proliferation, blockade of the ORN developmental pathway at the MASH1$^+$ cell stage, and eventually, cell death (Shou et al., 1999). Interestingly, GDF11 does not act via this mechanism: when we grew OE explant cultures in the presence or absence of GDF11 for 8 hr in vitro—a time when MASH1 expression is maximal under

normal culture conditions—we saw no effect of GDF11 on MASH1 expression (Figure 2B). (BMP4 treatment for this same time period, in contrast, results in almost complete loss of MASH1 expression [Shou et al., 1999]). Not only does GDF11 fail to target MASH1 for degradation, it also has no antiproliferative effect on MASH1-expressing progenitors: the percentage of MASH1$^+$ cells incorporating ^{3}H-TdR is unchanged by treatment with GDF11 (Figure 2C). Thus, GDF11 has a strong negative effect on neuronal progenitors, but not by acting on those which express MASH1.

The progeny of MASH1-expressing cells are INPs, the direct progenitors of ORNs (Figure 1F) and the most abundant progenitor cell type in OE explant cultures (Calof and Chikaraishi, 1989; DeHamer et al., 1994). Fibroblast growth factor 2 (FGF2) stimulates INP divisions, and essentially all of the increase it brings about in ^{3}H-TdR incorporation by cells in OE explant cultures at 48 hr in vitro can be ascribed to an effect on INPs (DeHamer et al., 1994; Shou et al., 2000). We reasoned that if GDF11 exerts its inhibitory effect on INPs, it might abrogate the effect of FGF2. Indeed, as shown in Figure 2D, treatment with GDF11 completely abolishes the stimulatory effect of FGF2 on INPs, strongly suggesting that GDF11 inhibits INP divisions.

To show such an action directly, we needed a means of marking INPs in culture. Since INPs express *Ngn1*, we used a transgenic mouse line, TgN1-2G, in which GFP is expressed under the control of *Ngn1* regulatory elements (Gowan et al., 2001). To verify that GFP marks the correct cells in the OE, we crossed the *TgN1-2G* allele onto a *Mash1*$^{-/-}$ background (these mice lack *Ngn1*-expressing cells in most of the OE [Figure 1G] [see also Cau et al., 1997]) and observed that GFP expression in the OE indeed disappeared (Figure 3A). We also verified that GFP and MASH1 are expressed in distinct cells in explant cultures of *TgN1-2G* OE (Figure 3B), as expected if GFP marks INPs.

With this confirmation, we then tested directly the effect of GDF11 on OE explants cultured from *TgN1-2G* embryos. As shown in Figure 3C, GDF11 treatment results in a 3-fold decrease in the number of GFP-expressing cells that develop over the course of 22 hr, in a manner that is completely blocked by follistatin. Because GDF11 has no effect on proliferation of the MASH1-expressing cells that give rise to INPs (Figures 2B and 2C), we concluded that the decrease in GFP-expressing cells caused by GDF11 reflects a loss, or failure to expand, of existing INPs.

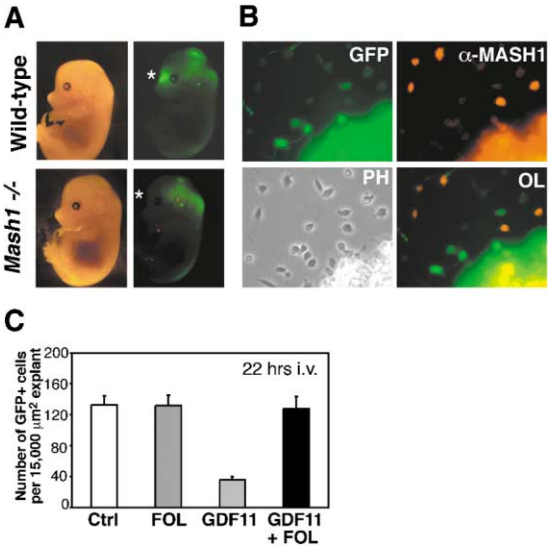

Figure 3. GDF11 Inhibits Development of INPs in Culture

(A) GFP expression in TgN1-2G transgenic mice requires *Mash1*. *Mash1*$^{+/-}$;*TgN1-2G*$^{+/-}$ mice were mated and offspring analyzed at E14.5 for expression of GFP. Asterisk indicates OE.

(B) MASH1 and GFP are expressed by different cells in OE cultures. OE explants from E14.5 *TgN1-2G*$^{+/-}$ embryos were grown 8 hr in vitro. MASH1 immunoreactivity was never seen in GFP$^+$ cells.

(C) Development of Ngn1$^+$, GFP$^+$ INPs is inhibited by GDF11. OE explants from *TgN1-2G*$^{+/-}$ embryos were cultured 22 hr in GDF11 (10 ng/ml), follistatin (FOL; 200 ng/ml), or both as indicated, and GFP$^+$ cells surrounding each explant counted. Error bars, SEM; $p < 0.05$, Dunnett test.

GDF11 Treatment Leads to Cell Cycle Arrest in INPs

The findings above indicated that GDF11 blocks the ORN developmental pathway at the INP stage, but left unclear the mechanism. To investigate this, we cultured OE explants from *TgN1-2G* embryos for 8, 16, or 24 hr, with and without added GDF11 (Figure 4A). Under control conditions, total cell number increased linearly between 8 and 24 hr, reflecting proliferation of both MASH1$^+$ progenitors and INPs, and the generation of ORNs. In GDF11-treated cultures, however, there was no increase in total cell number. Similarly, in control cultures the number of GFP$^+$ cells (presumed INPs) increased steeply from 8 to 16 hr and then began to plateau, reflecting division of INPs followed by their generation of terminally differentiated ORNs (Figure 4B) (Calof and Chikaraishi, 1989; DeHamer et al., 1994). In marked contrast, no increase in GFP$^+$ cell number occurred in GDF11-treated cultures, although similar numbers of INPs were present initially whether or not GDF11 had been applied (Figure 4B). As expected, MASH1-expressing progenitors, which normally decline in number during culture (Gordon et al., 1995), were unaffected by GDF11 treatment at any time point tested (Figure 4C).

The failure of INP numbers to increase in GDF11-treated cultures might be due to decreased INP proliferation, but could also be caused by an effect on INP survival. To test this, we performed TUNEL assays on OE explants grown for 19 hr in the presence of GDF11 (Holcomb et al., 1995). The fraction of INPs (GFP$^+$ cells) undergoing apoptosis was not significantly different in GDF11-treated cultures than in untreated controls (Figure 4D). This result supports the view that, in the presence of GDF11, INPs remain alive, but no longer progress through the cell cycle and therefore no longer generate ORNs.

If GDF11 acts by causing cell cycle arrest, then its effect might be reversible. To test this, we grew *TgN1-2G*$^{+/-}$ explants for 12 hr in GDF11, and then removed GDF11 from half of the cultures. Explants were maintained for an additional 18 hr, with ^{3}H-TdR added for the final 6 hr to label cells in S phase. In cultures from which GDF11 had been removed, more than twice as

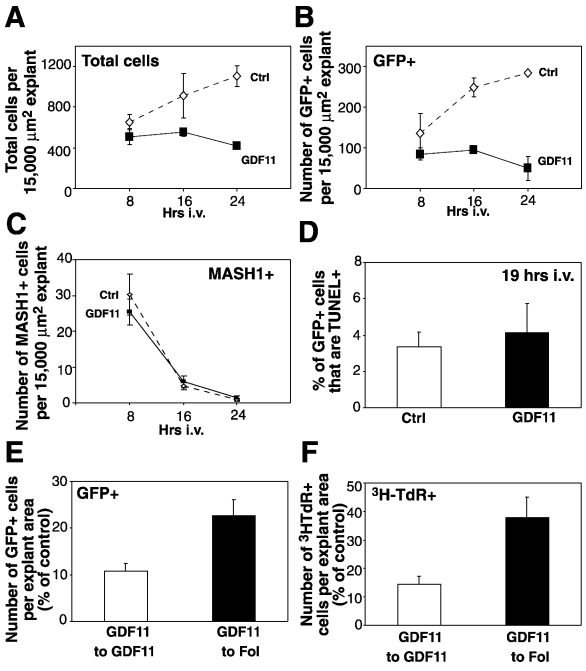

Figure 4. GDF11 Reversibly Inhibits Division of INPs

(A–C) OE explants from *TgN1-2G*$^{+/-}$ embryos were grown with or without GDF11 (20 ng/ml) and fixed at indicated times. Total migratory cells (A), GFP^{+} cells (B), and MASH1^{+} cells (C) surrounding individual explants were counted. (A) Error bars, SD; $p < 0.05$ for $t = 24$ hr; (B) Error bars, SD; $p < 0.05$ for $t = 16$ hr and $t = 24$ hr (Student's t test); (C) Error bars, SEM.

(D) GDF11 does not promote apoptosis of INPs. OE explants isolated from *TgN1-2G*$^{+/-}$ embryos were cultured with or without GDF11 (20 ng/ml) for 19 hr, processed for TUNEL, and the percentage of GFP^{+} cells that were TUNEL^{+} determined. Error bars, SEM.

(E and F) GDF11's effect on INPs is reversible. *TgN1-2G*$^{+/-}$ explants were treated with 20 ng/ml GDF11 for 12 hr, then GDF11 was removed and cultures re-fed with medium containing follistatin (100 ng/ml; "GDF11 to Fol") or 20 ng/ml GDF11 ("GDF11 to GDF11"). Control cultures had no factor added for the first 12 hr, then were switched to medium containing 100 ng/ml follistatin. Total GFP^{+} cells and ^{3}H-TdR^{+} cells surrounding each explant were counted. Error bars were calculated from the square root of the sum of the squares of fractional errors for control and experimental values. $p < 0.005$ for (E) and (F); Student's t test.

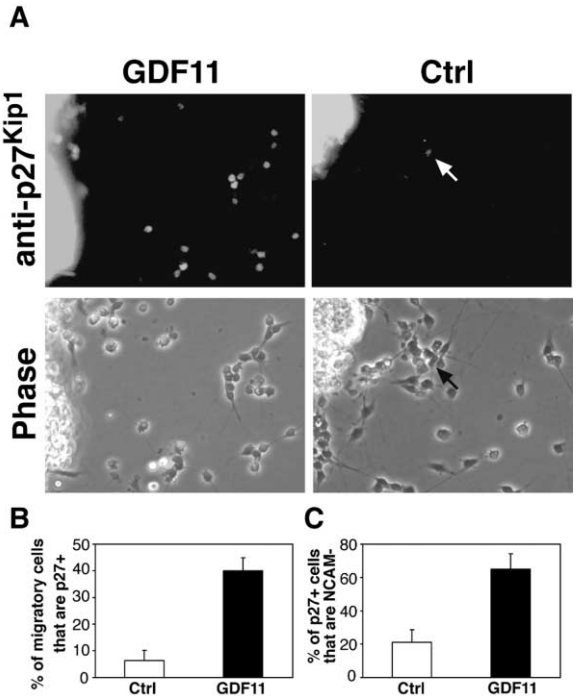

Figure 5. p27^{Kip1} Levels Are Increased in GDF11-Treated Neuronal Progenitor Cells

OE explants were cultured with or without GDF11 (20 ng/ml) for 14 hr and processed for p27^{Kip1} and NCAM immunoreactivity.

(A) Many migratory cells in GDF11-treated cultures express detectable levels p27^{Kip1}, almost none do in control (Ctrl; untreated) cultures (white arrow indicates a cell with low-level expression).

(B) Data in (A) were quantified as described in Experimental Procedures. Error bars, SEM; $p < 0.001$, Student's t test.

(C) Each p27^{+} cell in (B) was evaluated for NCAM immunoreactivity, and the percentage of p27^{+} cells that were NCAM negative (i.e., neuronal progenitors) calculated. Error bars, SEM; $p < 0.001$, Student's t test.

many GFP^{+} INPs were present at the end of the culture period (Figure 4E). Moreover, these cells were capable of dividing, as shown by incorporation of ^{3}H-TdR (Figure 4F). These results show that INPs are still present and viable in GDF11-treated cultures, but are reversibly arrested in the cell cycle.

We speculated that GDF11-induced cell cycle arrest was likely to occur in G1, a crucial phase of cell cycle control for many kinds of progenitors. The cyclin-dependent kinase inhibitor p27^{Kip1} has been implicated as a mediator of G1 phase cell cycle arrest induced by TGF-β (e.g., Polyak et al., 1994). Since the type I TGF-β receptor, ALK5, is also the likely signaling receptor for GDF11 (Federman et al., 2000), and since p27^{Kip1} is known to be involved in regulating proliferation of neuronal progenitors (Chen and Segil, 1999; Dyer and Cepko, 2001; Levine et al., 2000; Miyazawa et al., 2000), we hypothesized that GDF11-induced cell cycle arrest in INPs might be accompanied by increased expression of p27^{Kip1}. To test this idea, we grew OE explants for 14 hr in the presence or absence of GDF11 and then processed the cultures with an antibody to p27^{Kip1} (Figure 5). Indeed, in OE explants treated with GDF11, the percentage of migratory neuronal cells expressing detectable levels of p27^{Kip1} immunoreactivity was 10-fold higher than in untreated controls (Figure 5B), and the majority of these p27^{+} cells were NCAM-negative neuronal progenitors (Figure 5C). These findings strongly support the hypothesis that GDF11 arrests INPs in the G1 phase of the cell cycle, through a mechanism involving increased expression of p27^{Kip1}.

Increased Neurogenesis in Mice Lacking Functional *Gdf11*

To determine if endogenous GDF11 regulates OE neurogenesis in vivo, we disrupted the mouse *Gdf11* gene, inserting a *neo* cassette into exon 3, which encodes the mature peptide (Figure 6A). This allele (referred to as *Gdf11*^{tm2}) is expected to be functionally null, as it encodes an aberrant transcript in which codons for four of the seven cysteines critical for proper structure and function of TGF-βs are absent (Scheufler et al., 1999). Consistent with this expectation, the gross phenotype

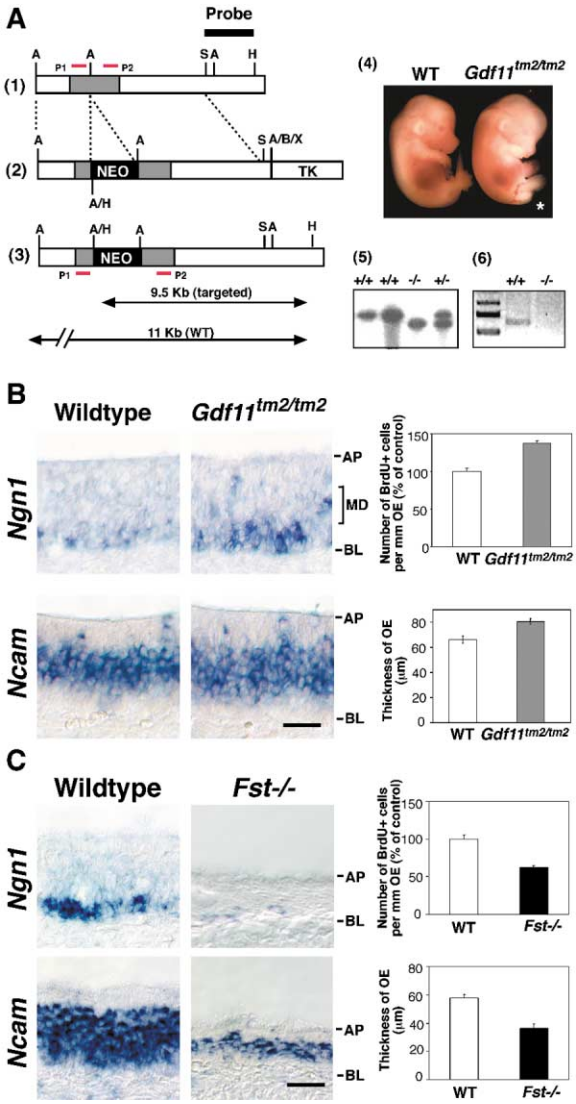

Figure 6. Disruption of Neurogenesis in Mice with Loss- or Gain-of-Function of *Gdf11*

(A) Analysis of *Gdf11*$^{tm2/tm2}$ mice. (1) *Gdf11* gene (wild-type allele). Lightly shaded box, exon 3; P1 and P2, locations of forward and reverse primers used for RT-PCR analysis in (6). "A," *ApaI*; "B," *BamHI*; "H," *HindIII*; "N," *NotI*; "S," *SalI*; "X," *XbaI*. (2) Targeting vector. NEO, PGKneopA cassette; TK, MC1-thymidine kinase cassette. (3) Targeted allele. Double-headed arrows indicate expected lengths of HindIII fragments for wild-type and targeted alleles detected using probe indicated in (1). A HindIII site is introduced into the targeted allele by the PGKneopA cassette. (4) Wild-type and *Gdf11*$^{tm2/tm2}$ littermates at E15.5; note lack of tail in *Gdf11*$^{tm2/tm2}$ embryo (asterisk). (5) Southern analysis of HindIII-digested DNAs from wild-type (+/+), knockout (−/−), and heterozygous (+/−) littermates from a litter obtained by intercrossing *Gdf11*$^{tm2/+}$ mice, using probe indicated in (1). (6) Absence of wild-type *Gdf11* mRNA in *Gdf11*$^{tm2/tm2}$ animals. Total RNA, extracted from olfactory turbinates of E15.5 *Gdf11*$^{tm2/tm2}$ embryos and wild-type littermates, was reverse transcribed and resulting cDNAs analyzed by PCR to detect wild-type *Gdf11* transcript. P1: 5′-CTCCGGCCAGTGCGAATACA-3′; P2: 5′-TCCACAGCCAAGGTGAGAGG-3′. A ~600 bp fragment is generated from wild-type cDNA, but not cDNA of *Gdf11*$^{tm2/tm2}$ embryos. Control PCR using primers for mouse *Hprt* (Shou et al., 2000) demonstrated that equal amounts of cDNA were present in each reaction (data not shown).

(B) *Gdf11*$^{tm2/tm2}$ mice exhibit increased OE neurogenesis. Dams were injected twice with BrdU and OE cryosections from E14.5 wild-type and *Gdf11*$^{tm2/tm2}$ littermate embryos processed for BrdU immunoreactivity or ISH with probes for *Ngn1* and *Ncam*. BrdU$^+$ cells/mm septal OE were counted in sections from four wild-type and four *Gdf11*$^{tm2/tm2}$ littermate embryos; data were normalized to wild-type values. Error bars were calculated as described for Figures 4E and 4F; $p < 0.05$, Student's t test. Thickness of septal OE was measured (using NIH Image) in sections from three wild-type and four *Gdf11*$^{tm2/tm2}$ littermates. Error bars, SEM; $p < 0.05$, Student's t test.

(C) Mice lacking a functional *Follistatin* gene show decreased OE neurogenesis. Dams were injected once with BrdU and cryosections of OE from E17.5 wild-type and *Fst*$^{-/-}$ littermates analyzed as described for (B). BrdU-immunoreactive cells in septal OE were counted in sections from two wild-type and two *Fst*$^{-/-}$ littermates ($p < 0.05$, Student's t test). Thickness of septal OE was measured as described in (B); four wild-type and four *Fst*$^{-/-}$ littermates were examined ($p < 0.05$, Student's t test).

of *Gdf11*$^{tm2/tm2}$ mice is identical to that reported for an independently generated null allele of *Gdf11* (McPherron et al., 1999): all *Gdf11*$^{tm2/tm2}$ mice die within 24 hr of birth, exhibiting sacral agenesis, renal abnormalities, aberrant positioning of the hindlimb bud, and anterior transformations of vertebral segments with concurrent loss of vertebrae from sacral and caudal regions (Figure 6A and data not shown).

We then analyzed OE neurogenesis in *Gdf11*$^{tm2/tm2}$ mice. Since removal of an antineurogenic signal would be expected to result in an increase in progenitor cell proliferation, we administered BrdU to pregnant dams and counted BrdU-incorporating cells in horizontal sections of septal OE from *Gdf11*$^{tm2/tm2}$ embryos and their wild-type littermates. As predicted, a significant increase in the number of BrdU$^+$ cells was observed in the OE of animals lacking functional *Gdf11*: 37% more BrdU$^+$ cells are present in the OE of *Gdf11*$^{tm2/tm2}$ animals than in wild-type OE (Figure 6B). This increase is even more dramatic if the middle layers of the OE (which normally contain very few proliferating cells) are considered separately: the middle third of the OE of *Gdf11*$^{tm2/tm2}$ animals contains an average of 97 ± 8.7 [SD] BrdU$^+$ cells per millimeter, versus 39 ± 13.2 [SD] BrdU$^+$ cells per millimeter in wild-type littermates, an increase of 147%. In addition, septal OE as a whole is also thicker (by 22%) in *Gdf11*$^{tm2/tm2}$ animals (Figure 6B). (This increase is unlikely to be an artifact resulting from changes in nasal pit size and/or OE surface area, since the gross morphology of the nasal cavity and olfactory turbinates is similar between wild-type and *Gdf11*$^{tm2/tm2}$ animals; moreover, comparisons of OE size between wild-type and mutant littermates showed no significant quantitative differences [length of nasal septum lined by OE: wild-type, 1.6 ± 0.11 mm; *Gdf11*$^{tm2/tm2}$, 1.69 ± 0.1 mm; linear dimension of olfactory turbinate surface lined by OE: wild-type, 7.4 ± 1.3 mm; *Gdf11*$^{tm2/tm2}$, 7.28 ± 0.74 mm; mean ± SD of data from two litters]).

As described earlier, the effects of GDF11 in vitro appear to be exerted specifically on *Ngn1*-expressing INPs (Figures 2 and 3). In agreement with such an action, in situ hybridization experiments revealed a consistent increase in *Ngn1*-expressing cells in the OE of *Gdf11*$^{tm2/tm2}$ animals (Figure 6B). Notably, more *Ngn1*-expressing cells were seen in the middle cell layers of the OE, the same layers that had also been noted to contain a disproportionately large increase in BrdU-

incorporating cells (see above). We also examined *Mash1* expression in the OE, both by in situ hybridization and with a monoclonal antibody to MASH1, and failed to detect any significant change between *Gdf11*$^{tm2/tm2}$ animals and wild-types (there were 258 ± 58 [SD] MASH1-immunopositive cells per millimeter in wild-type OE, versus 286 ± 32 [SD] MASH1-immunopositive cells per millimeter in *Gdf11*$^{tm2/tm2}$ OE). Together, these results indicate that the overall increase in proliferating cells in *Gdf11*$^{tm2/tm2}$ OE is due specifically to an increase in the number of INPs. That these supernumerary progenitors go on to give rise to neurons was demonstrated by an increase in *Ncam*-expressing cells in *Gdf11*$^{tm2/tm2}$ OE: the *Ncam*-expressing cell layer is thicker by 20% (9 μm, about the diameter of one ORN) in *Gdf11*$^{tm2/tm2}$ OE than in wild-types. (The average thickness of the *Ncam*$^{+}$ layer of the OE was measured in sections hybridized with the *Ncam* probe, as illustrated in Figure 6B; values obtained were 33.05 ± 1.04 μm [SEM] for wild-type OE, versus 42.49 ± 0.98 [SEM] for *Gdf11*$^{tm2/tm2}$ OE [$p < 0.05$, Student's t test]). Thus, not only is proliferation of INPs increased in *Gdf11*$^{tm2/tm2}$ animals, so is production of differentiated neurons.

Decreased Neurogenesis in Mice Lacking Follistatin, a GDF11 Antagonist

If GDF11 truly functions as an endogenous negative regulator of neurogenesis in the OE, then an increase in GDF11 activity would be expected to result in a decrease in neurogenesis, to below normal levels. Follistatin has been shown to antagonize GDF11 activity in *Xenopus* animal cap assays (Gamer et al., 1999), and in OE cultures, follistatin is able to antagonize the antineurogenic effect of GDF11 on INPs (Figure 3). Since *Fst* mRNA is also expressed within the OE (Figure 1D), we reasoned that mice lacking a functional *Fst* gene might show evidence of increased GDF11 activity in the OE. This idea was tested by examining the OE of *Fst*$^{-/-}$ embryos (*Fst*$^{-/-}$ mice die at birth [Matzuk et al., 1995]), using markers for OE neuronal cells and BrdU incorporation to detect proliferating progenitors. The data are shown in Figure 6C. In situ hybridization for *Ngn1* and *Ncam* showed large decreases in expression of both markers, indicating that production of both INPs and ORNs is profoundly decreased in *Fst*$^{-/-}$ OE. Strikingly, we also observed a 37% decrease in the number of BrdU-incorporating cells and a 38% decrease in OE thickness in *Fst*$^{-/-}$ animals. These results indicate that the action of follistatin is required for normal levels of neurogenesis in the OE. Since follistatin by itself has no effect on neurogenesis when tested in OE explants (Figure 3), these findings also suggest that the decrease of neurogenesis in *Fst*$^{-/-}$ animals is the result of increased activity of a molecule antagonized by follistatin, such as GDF11.

Discussion

Negative Autoregulation of Neurogenesis by Endogenous Signaling Molecules

How tissues reach and maintain their appropriate sizes has been the subject of speculation for many years. Almost 40 years ago, Bullough put forward the hypothesis that tissues produce growth-inhibitory signals, called "chalones," the local concentrations of which directly reflect the mass of the tissue in which they are produced (Bullough, 1965). Such signals were proposed to halt cell proliferation when appropriate tissue size had been reached, thereby maintaining the cell number appropriate for tissue function. The discovery of GDF8 (myostatin), a signaling molecule of the TGF-β superfamily which is both made by developing muscle cells and inhibits their proliferation, has validated this idea (Lee and McPherron, 1999).

For several years, we have sought to identify the molecular signal(s) that mediate feedback inhibition of neurogenesis in the OE. Recently, we suggested that BMPs, and in particular BMP4, may provide such a signal. BMP4 is expressed in OE and, in vitro, blocks the ORN lineage at the MASH1^{+} progenitor cell stage (Shou et al., 1999). Although these observations make BMP4 a plausible candidate for a feedback inhibitor of neurogenesis, the additional facts that (1) *Bmp4* is expressed not only in OE proper, but also elsewhere in the nasal region (e.g., in OE stroma); and (2) BMP4 effects on the ORN lineage are complex, with BMP4 actually promoting OE neurogenesis at low concentration by supporting ORN survival (Shou et al., 2000), prompted our search for other TGF-βs that might be better candidates for the endogenous negative growth signal. This led us to investigate GDF11.

The data presented here demonstrate that GDF11 is a critical endogenous inhibitor of OE neurogenesis. Its effects in vitro are directed at a specific stage of transit-amplifying progenitors, the *Ngn1*-expressing INPs. GDF11 does not drive INPs into apoptosis, as BMPs do with some neuronal progenitors (e.g., Shou et al., 1999), nor does it reduce progenitor cell number by promoting neuronal differentiation, another mechanism by which BMPs have been reported to act (e.g., Li et al., 1998). Instead, GDF11 reversibly blocks INP divisions (Figure 4), and this is associated with increased expression of the cyclin-dependent kinase inhibitor, p27^{Kip1} (Figure 5). In vivo, lack of *Gdf11* function results in an increase in proliferating, *Ngn1*-expressing INPs and an approximate 20% increase in neuron number within the epithelium (Figure 6). Conversely, in mice lacking a functional *follistatin* gene (Matzuk et al., 1995), which encodes a secreted GDF11 antagonist (Gamer et al., 1999), there is a substantial *decrease* in OE neurogenesis. This is evident as a decrease in both OE thickness and the number of proliferating progenitors within the OE, as well as by decreases in *Ngn1*$^{+}$ INPs and *Ncam*-expressing ORNs (Figure 6). Together, these observations demonstrate that the GDF11 and follistatin are both of crucial importance in regulating OE neurogenesis, and suggest that follistatin's role in vivo, at least in part, is to modulate the activity of endgenous GDF11. (Since follistatin also binds with high affinity to activin [Schneyer et al., 1994] and antagonizes activin's biological activities [Nakamura et al., 1990], it remains possible that endogenous activin [Feijen et al., 1994] may also interact with follistatin in modulating OE neurogenesis. This possibility is currently under investigation in our laboratory.)

It is not known if the CNS controls neuron number using a mechanism similar to the feedback inhibitory mechanism we have proposed for OE. An important

part of determining whether such a mechanism might operate will be to test likely signaling molecules for their potential role(s) as autocrine-negative regulators of neurogenesis. Significantly, both GDF11 and follistatin show widespread expression in the CNS (data not shown) (Feijen et al., 1994; Nakashima et al., 1999; Roberts and Barth, 1994), including regions such as the dentate gyrus of the hippocampus, the external granule layer of the cerebellum, and neural retina, where neurogenesis is known to be tightly controlled by cell interactions (e.g., Parent et al., 1997; Sloviter et al., 1996). Given these facts, it is reasonable to hypothesize that GDF11 and follistatin may be important players in a process of feedback inhibition of neurogenesis that could act to regulate neuron number during development (and, potentially, regeneration) of the CNS.

Regulation of Neuron Number by GDF11

Although GDF11 clearly acts as a negative regulator of neurogenesis in the OE, we found no evidence that it affects neuronal cell survival or fate. All neuronal cell types are still present in the OE of *Gdf11*$^{tm2/tm2}$ mice; only their numbers, and consequently the overall thickness of the OE, are altered (Figure 6). Thus, GDF11, like the chalones proposed by Bullough (1965), appears to act in an autocrine fashion as a dynamic negative regulator of OE tissue size.

Data from in vitro experiments suggest that GDF11 may induce cell cycle arrest of INPs by increasing the expression of the cyclin-dependent kinase inhibitor, p27^{Kip1} (Figure 5). In fact, the OE of *p27*$^{Kip1-/-}$ mice has been reported to contain an increased number of BrdU-incorporating cells (Legrier et al., 2001), raising the possibility that p27^{Kip1} is a major downstream target of GDF11 in vivo. In this light, it may be significant that the percentage increase in thickness of the OE in *Gdf11*$^{tm2/tm2}$ mice (~22%) is similar to the increase in brain size (~18%) observed in mice with targeted inactivation of the *p27*^{Kip1} gene (Fero et al., 1996). In considering the importance of this effect, it is notable that such an increase in size in a neural tissue can profoundly disrupt function. For example, the modest increase in hair cell number in the inner ear of *p27*$^{Kip1-/-}$ animals (23% increase in inner hair cells; 36% in outer hair cells) results in profound hearing impairment (Chen and Segil, 1999). Such findings emphasize how important control of neuron number is to nervous system function.

Is GDF11 Important for Neuronal Regeneration?

The OE is one of the few regions of the mammalian nervous system with the capacity for true neuronal regeneration, and the action of GDF11 on INPs may be of special significance in regulating the temporal dynamics of this process. INPs function as transit-amplifying cells in the ORN lineage, proliferating in response to extrinsic cues but remaining committed to a neuronal (ORN) fate (DeHamer et al., 1994). In vivo, death of ORNs provides such a cue, causing INP proliferation to increase rapidly and remain elevated until neuron number is restored (reviewed in Calof et al., 1996a). Thus, in the OE, as in many regenerating tissues, transit-amplifying cells, by rapidly altering their proliferation in response to extrinsic cues, provide the capacity for rapid changes in the sizes of differentiated cell populations in response to changing environmental demands (Hall and Watt, 1989; Potten and Loeffler, 1990). By inducing a reversible state of growth inhibition, GDF11 may play an important role in maintaining the INP population in an appropriate state to respond rapidly to environmental signals. GDF11's ability to induce p27^{Kip1} is likely to be of importance in this process, as p27^{Kip1}has been shown recently to be important in determining numbers of transit-amplifying progenitors elsewhere in the nervous system (Doetsch et al., 2002).

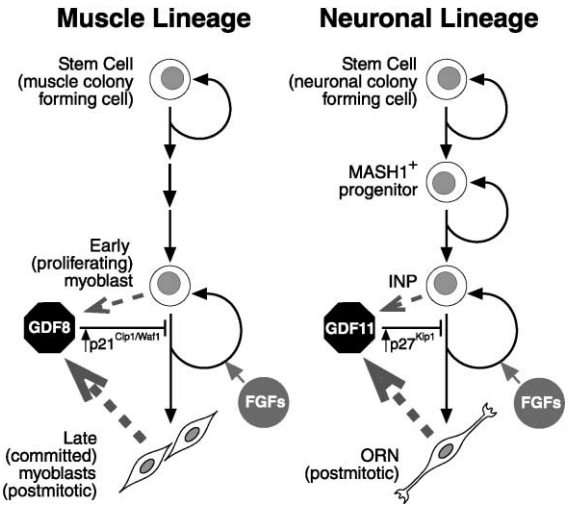

Figure 7. Parallels between the Regulation of Myogenesis and Neurogenesis

Skeletal muscle lineage (Miller et al., 1999) and the neuronal lineage of the OE are illustrated. Cell types in which GDF8 and GDF11 are produced, and upon which they act (discussed in text), are indicated.

Parallels between Neurogenesis and Myogenesis

A striking finding of the present study is the degree to which mechanisms of feedback regulation of tissue size appear to have been conserved between neuronal and muscle lineages (Figure 7). In muscle, not only does GDF8 exert the same sort of growth inhibitory effect as GDF11 in the OE (Lee and McPherron, 1999), GDF8 also appears to utilize an analogous mechanism: inducing G1 phase arrest in early myoblasts (Thomas et al., 2000), which are FGF-stimulated transit-amplifying cells similar to INPs (Clegg et al., 1987). Furthermore, GDF8-induced cell cycle arrest is characterized by an increase in expression of p21$^{Cip1/Waf1}$ (Thomas et al., 2000), a homolog of p27^{Kip1} that acts similarly to cause cell cycle arrest. Interestingly, such mechanisms may be utilized not only in vertebrate tissues, but also in invertebrates: the recent description of *Drosophila* GDF-11/GDF-8 and activin homologs, which are highly expressed in muscle, glial, and neuronal progenitors (Lo and Frasch, 1999), suggests that these TGF-βs may function as negative regulators of cell division in the same *Drosophila* tissues as those in which they act in vertebrates. Altogether, these results suggest that fundamental mechanisms of tissue size regulation are evolutionarily ancient and thus are likely to be of great importance as control mechanisms during development and regeneration.

Experimental Procedures

Materials

Recombinant human GDF8 and GDF11 were from Genetics Institute/Wyeth. GDF11was used as conditioned medium collected from CHO cells stably transfected with human *Gdf11* cDNA (GenBank #AF100907); GDF11 concentration was quantified by immunoblotting. Follistatin was obtained through the National Hormone & Pituitary Program and A.F. Parlow, Harbor-UCLA Medical Center (Torrance, CA). Recombinant human FGF2 (157 aa form) was from R&D Systems.

Animals

Day of vaginal plug detection was designated day 0.5 of embryonic development. *Mash1*$^{+/-}$ mice were maintained on a CD-1 (Charles River) background, where the OE phenotype is fully penetrant (our observations and Cau et al. [1997]). *TgN1-2G* transgenic mice were maintained as homozygotes on a CD-1 background; to obtain OE for tissue culture, *TgN1-2G*$^{+/+}$ males were mated with CD-1 females and the resulting offspring used. *Fst*$^{+/-}$ animals were maintained on an inbred C57BL/6J background. *Fst*$^{-/-}$ animals were genotyped using primers to the inserted human HPRT sequences (targeted allele: forward primer, 5′-GGCAAAGGATGTGATACGTGGAAG-3′; reverse primer, 5′-CCAGTTTCACTAATGACACAAACATG-3′) and sequences within exon 2 and 3 of *Fst* (wild-type allele: forward primer, 5′-CTGAGCACCTCATGGACCGA-3′; reverse primer, 5′-CAC ATTCGTTGCGGTAGGTT-3′). The *Fst* wild-type allele was detected as an ~700 bp fragment and the targeted allele as a ~850 bp fragment.

Mice deficient in *Gdf11* (*Gdf11*$^{tm2/tm2}$ mice) were generated by gene targeting. *Gdf11* clones were isolated from a 129/Sv mouse genomic DNA λ phage library (Stratagene). The targeting construct (Figure 6A) was generated by inserting a neomycin resistance gene under the control of the PGK promoter (PGKneopA) into the *ApaI* site in the third coding exon. The 5′and 3′ flanks consist, respectively, of 1.1 and 6.0 kb *ApaI* fragments. An MC1-thymidine kinase cassette (MC1tkpA) is downstream of the 3′ flank. Plasmid sequences were released by digestion with *SalI*, and the targeting vector electroporated into RW-4 ES cells (Genome Systems). Correctly targeted ES clones were identified by Southern blot analysis, and two independent clones introduced into the mouse germline by blastocyst injection (Hogan et al., 1994). Heterozygous mice appeared normal and were intercrossed to obtain homozygous mutant mice. *Gdf11*$^{tm2/+}$ (CD1,F1) mice were generated by crossing *Gdf11*$^{tm2/+}$ mice on a 129/SV background with CD-1 females. *Gdf11*$^{tm2/tm2}$ embryos and their littermates used in this study were generated by intercrossing *Gdf11*$^{tm2/+}$ (CD1,F1) males and females. Animals were genotyped using a 3-primer PCR analysis of genomic DNA, with forward and reverse primers spanning the PGKneo cassette in the targeted allele (5′-CGCTGCTGCCGATATCCTCT-3′ forward primer, 5′-GCCTTCTT GACGAGTTCTTC-3′ reverse primer), and a third primer (5′-GCC TTCTTGACGAGTTCTTC-3′) in the neomycin gene. The *Gdf11* wild-type allele was detected as a ~280 bp product and the *Gdf11*^{tm2} allele as a ~500 bp product.

In Situ Hybridization, Immunofluorescence, and TUNEL Analyses

For immunofluorescence on sections, pregnant dams were injected with BrdU (50 μg/gm body weight), at 1 hr (single injection) or 1 and 2 hr (double injection) prior to sacrifice and processing of tissue. Embryos were dissected and heads fixed in 4% paraformaldehyde, 5% sucrose in phosphate-buffered saline (PBS) for 2–3 hr at room temperature, embedded and cryosectioned in the horizontal plane at 12 μm. Sections were incubated with rat anti-BrdU (clone BU1/75 [ICR1], Harlan), detected with Texas Red-conjugated goat anti-rat IgG (Jackson). MASH1- and NCAM-expressing cells were detected as described previously (DeHamer et al., 1994; Gordon et al., 1995; Shou et al., 1999).

For in situ hybridyzation (ISH), embryos were dissected in cold PBS and heads fixed in 4% paraformaldehyde in PBS (pH 7.2) overnight at 4°C, rinsed, and then cryosectioned at 20 μm. ISH on sections and wholemount ISH were performed as described (Kawauchi et al., 1999; Shou et al., 2000). Digoxigenin-labeled cRNA probes were: 1.2 kb mouse *Gdf11* partial cDNA (bp 229–1218 of coding region; Genbank #AH006982) plus ~500 bp of 3′ noncoding sequence; bases 1201–1835 of mouse *Gdf8* 3′ UTR (GenBank #NM010834); 437 bp mouse *Alk5* (87–511 bp of Genbank #NM009307); 308 bp mouse *ActRIIb* (119–427 bp of Genbank #M84120); 770 bp partial mouse *fst* cDNA (Albano et al., 1994); *Ngn1* (1.2 kb fragment of rat *Ngn1* gene [Ma et al., 1996]); and *Mash1* (2.0 kb fragment of mouse *Mash1* gene including coding region and 3′UTR [Guillemot and Joyner, 1993]). Hybridization was detected using alkaline phosphatase-conjugated sheep anti-digoxigenin Fab fragments, followed by BCIP/NBT according to manufacturer's instructions (Roche).

For quantification of BrdU- and MASH1-immunopositive cell numbers, as well as overall OE thickness and thickness of *Ncam*-expressing cell layers, multiple adjacent fields of OE lining the nasal septum (chosen because this is an uncurved structure with an OE lining of regular thickness) were evaluated at 400× magnification. In comparing wild-type and transgenic animals, sections from similar levels along the dorsal-ventral axis were chosen for analysis in all cases.

To detect p27^{Kip1}, cultures were fixed and processed as described for MASH1 immunostaining (Shou et al., 1999); the primary antibody (monoclonal anti-p27^{Kip1}; clone 57; BD Transduction Laboratories) was detected using rabbit anti-mouse IgG1 (Harland) followed by AlexaFluor 594-conjugated goat anti-rabbit IgG (Molecular Probes). Confirmation that this antibody recognizes authentic p27^{Kip1} in OE cultures was obtained by immunoblotting (data not shown). To quantify p27^{Kip1} immunoreactivity, individual cells were imaged under rhodamine optics with a 40× oil objective (Zeiss) using a cooled CCD digital camera (Diagnostic Instruments SP100, 1315 × 1035 pixel resolution). Raw data files were imported to NIH ImageJ v.1.28 and total migratory cells and cells with mean fluorescence intensities ≥25 ("p27^{+} cells") counted (mean background intensity for controls = 3.7 ± 0.2; for GDF11-treated culture = 3.5 ± 0.2). TUNEL staining of cultures was performed as described (Holcomb et al., 1995), using biotin-16-dUTP detected with Texas Red-conjugated Neutravidin (Molecular Probes).

Primary OE Cultures

OE explant cultures were prepared as described previously (DeHamer et al., 1994; Shou et al., 1999) and grown in vitro for the indicated times. ^{3}H-thymidine (^{3}H-TdR; 60–80 Ci/mmol, 1 mCi/ml, ICN) was applied at the following concentrations: 1.5 μCi/ml for the final 6 hr in explants cultured for 22 hr, 5 μCi/ml for the final 2 hr in explants cultured for 8 hr, and 0.1 μCi/ml for the final 24 hr in explants cultured for 48 hr. Cultures were fixed and processed for autoradiography as described previously (DeHamer et al., 1994; Shou et al., 1999). For comparison of labeled migratory cell numbers among different explants in a given experiment, total numbers of cells surrounding each explant were counted and the size of the explant measured using NIH Image. Because explants are irregular in area, the number of ^{3}H-TdR^{+} cells for each explant was normalized to an area value of 15,000 μm^{2}, the average size of explants in these cultures (cf. DeHamer et al., 1994).

Acknowledgments

This work was supported by grants to A.L.C. from the NIH (DC03583 and HD38761) and the March of Dimes. S.I. and K.M.L. are supported by NIH grant AR44528. The authors thank Tony Celeste for probes to *Alk5*, *ActRIIb*, and *Gdf8*; Martin Matzuk for *Fst*$^{+/-}$ mice; and members of the Calof lab and Arthur Lander for helpful comments.

Received: July 8, 2002
Revised: December 9, 2002

References

Albano, R.M., Arkell, R., Beddington, R.S., and Smith, J.C. (1994). Expression of inhibin subunits and follistatin during postimplantation mouse development: decidual expression of activin and expression of follistatin in primitive streak, somites and hindbrain. Development *120*, 803–813.

Bullough, W.S. (1965). Mitotic and functional homeostasis: a speculative review. Cancer Res. *25*, 1683–1727.

Calof, A.L., and Chikaraishi, D.M. (1989). Analysis of neurogenesis in a mammalian neuroepithelium: proliferation and differentiation of an olfactory neuron precursor in vitro. Neuron *3*, 115–127.

Calof, A.L., Hagiwara, N., Holcomb, J.D., Mumm, J.S., and Shou, J. (1996a). Neurogenesis and cell death in the olfactory epithelium. J. Neurobiol. *30*, 67–81.

Calof, A.L., Holcomb, J.D., Mumm, J.S., Haglwara, N., Tran, P., Smith, K.M., and Shelton, D. (1996b). Factors affecting neuronal birth and death in the mammalian olfactory epithelium. Ciba Found. Symp. *196*, 188–205.

Calof, A.L., Mumm, J.S., Rim, P.C., and Shou, J. (1998). The neuronal stem cell of the olfactory epithelium. J. Neurobiol. *36*, 190–205.

Calof, A., Bonnin, A., Crocker, C., Kawauchi, S., Murray, R., Shou, J., and Wu, H.-H. (2002). Progenitor cells of the olfactory receptor neuron lineage. Microsc. Res. Tech. *58*, 176–188.

Cau, E., Gradwohl, G., Fode, C., and Guillemot, F. (1997). Mash1 activates a cascade of bHLH regulators in olfactory neuron progenitors. Development *124*, 1611–1621.

Caviness, V.S., Takahashi, T., and Nowakowski, R.S. (1995). Numbers, time and neocortical neuronogenesis: a general developmental and evolutionary model. Trends Neurosci. *18*, 379–383.

Chen, P., and Segil, N. (1999). p27(Kip1) links cell proliferation to morphogenesis in the developing organ of Corti. Development *126*, 1581–1590.

Clegg, C.H., Linkhart, T.A., Olwin, B.B., and Hauschka, S.D. (1987). Growth factor control of skeletal muscle differentiation: commitment to terminal differentiation occurs in G1 phase and is repressed by fibroblast growth factor. J. Cell Biol. *105*, 949–956.

DeHamer, M.K., Guevara, J.L., Hannon, K., Olwin, B.B., and Calof, A.L. (1994). Genesis of olfactory receptor neurons in vitro: regulation of progenitor cell divisions by fibroblast growth factors. Neuron *13*, 1083–1097.

Doetsch, F., Verdugo, J.M., Caille, I., Alvarez-Buylla, A., Chao, M.V., and Casaccia-Bonnefil, P. (2002). Lack of the cell-cycle inhibitor p27Kip1 results in selective increase of transit-amplifying cells for adult neurogenesis. J. Neurosci. *22*, 2255–2264.

Dyer, M.A., and Cepko, C.L. (2001). p27Kip1 and p57Kip2 regulate proliferation in distinct retinal progenitor cell populations. J. Neurosci. *21*, 4259–4271.

Federman, S.M., Thies, R.S., Chen, T., Gamer, L., Wolfman, N.M., and Celeste, A.J. (2000). Binding of GDF-8 to the activin type IIB receptor is blocked by the GDF-8 propeptide and enhanced by the activin binding protein, follistatin. J. Bone Miner. Res. *15*, S103.

Feijen, A., Goumans, M.J., and van den Eijnden-van Raaij, A.J. (1994). Expression of activin subunits, activin receptors and follistatin in postimplantation mouse embryos suggests specific developmental functions for different activins. Development *120*, 3621–3637.

Fero, M.L., Rivkin, M., Tasch, M., Porter, P., Carow, C.E., Firpo, E., Polyak, K., Tsai, L.H., Broudy, V., Perlmutter, R.M., et al. (1996). A syndrome of multiorgan hyperplasia with features of gigantism, tumorigenesis, and female sterility in p27(Kip1)-deficient mice. Cell *85*, 733–744.

Gamer, L.W., Wolfman, N.M., Celeste, A.J., Hattersley, G., Hewick, R., and Rosen, V. (1999). A novel BMP expressed in developing mouse limb, spinal cord, and tail bud is a potent mesoderm inducer in Xenopus embryos. Dev. Biol. *208*, 222–232.

Gordon, M.K., Mumm, J.S., Davis, R.A., Holcomb, J.D., and Calof, A.L. (1995). Dynamics of MASH1 expression in vitro and in vivo suggest a non-stem cell site of MASH1 action in the olfactory receptor neuron lineage. Mol. Cell. Neurosci. *6*, 363–379.

Gowan, K., Helms, A.W., Hunsaker, T.L., Collisson, T., Ebert, P.J., Odom, R., and Johnson, J.E. (2001). Crossinhibitory activities of Ngn1 and Math1 allow specification of distinct dorsal interneurons. Neuron *31*, 219–232.

Guillemot, F., and Joyner, A.L. (1993). Dynamic expression of the murine Achaete-Scute homologue Mash-1 in the developing nervous system. Mech. Dev. *42*, 171–185.

Guillemot, F., Lo, C.-C., Johnson, J.E., Auerbach, A., Anderson, D.J., and Joyner, A.L. (1993). Mammalian achaete-scute homolog 1 is required for the early development of olfactory and autonomic neurons. Cell *75*, 463–476.

Hall, P.A., and Watt, F.M. (1989). Stem cells: the generation and maintenance of cellular diversity. Development *106*, 619–633.

Hogan, B., Beddington, R., Costantini, F., and Lacy, E. (1994). Manipulating the Mouse Embryo: A Laboratory Manual (Cold Spring Harbor, NY: Cold Spring Harbor Laboratory Press).

Holcomb, J.D., Mumm, J.S., and Calof, A.L. (1995). Apoptosis in the neuronal lineage of the mammalian olfactory epithelium: regulation in vivo and in vitro. Dev. Biol. *172*, 307–323.

Kauffman, S.L. (1968). Lengthening of the generation cycle during embryonic differentiation of the mouse neural tube. Ex.l Cell Res. *49*, 420–424.

Kawauchi, S., Takahashi, S., Nakajima, O., Ogino, H., Morita, M., Nishizawa, M., Yasuda, K., and Yamamoto, M. (1999). Regulation of lens fiber cell differentiation by transcription factor c-Maf. J. Biol. Chem. *274*, 19254–19260.

Lee, S.J., and McPherron, A.C. (1999). Myostatin and the control of skeletal muscle mass. Curr. Opin. Genet. Dev. *9*, 604–607.

Lee, S.J., and McPherron, A.C. (2001). Regulation of myostatin activity and muscle growth. Proc. Natl. Acad. Sci. USA *98*, 9306–9311.

Legrier, M.E., Ducray, A., Propper, A., Chao, M., and Kastner, A. (2001). Cell cycle regulation during mouse olfactory neurogenesis. Cell Growth Differ. *12*, 591–601.

Levine, E.M., Close, J., Fero, M., Ostrovsky, A., and Reh, T.A. (2000). p27(Kip1) regulates cell cycle withdrawal of late multipotent progenitor cells in the mammalian retina. Dev. Biol. *219*, 299–314.

Li, W., Cogswell, C.A., and LoTurco, J.J. (1998). Neuronal differentiation of precursors in the neocortical ventricular zone is triggered by BMP. J. Neurosci. *18*, 8853–8862.

Lo, P.C., and Frasch, M. (1999). Sequence and expression of myoglianin, a novel Drosophila gene of the TGF-beta superfamily. Mech. Dev. *86*, 171–175.

Ma, Q., Kintner, C., and Anderson, D.J. (1996). Identification of neurogenin, a vertebrate neuronal determination gene. Cell *87*, 43–52.

Matzuk, M.M., Lu, N., Vogel, H., Sellheyer, K., Roop, D.R., and Bradley, A. (1995). Multiple defects and perinatal death in mice deficient in follistatin. Nature *374*, 360–363.

McPherron, A.C., Lawler, A.M., and Lee, S.J. (1997). Regulation of skeletal muscle mass in mice by a new TGF-beta superfamily member. Nature *387*, 83–90.

McPherron, A.C., Lawler, A.M., and Lee, S.J. (1999). Regulation of anterior/posterior patterning of the axial skeleton by growth/differentiation factor 11. Nat. Genet. *22*, 260–264.

Miller, J.B., Schaefer, L., and Dominov, J.A. (1999). Seeking muscle stem cells. Curr. Top. Dev. Biol. *43*, 191–219.

Miyazawa, K., Himi, T., Garcia, V., Yamagishi, H., Sato, S., and Ishizaki, Y. (2000). A role for p27/Kip1 in the control of cerebellar granule cell precursor proliferation. J. Neurosci. *20*, 5756–5763.

Mumm, J.S., Shou, J., and Calof, A.L. (1996). Colony-forming progenitors from mouse olfactory epithelium: evidence for feedback regulation of neuron production. Proc. Natl. Acad. Sci. USA *93*, 11167–11172.

Murray, R.C., Navi, D., Fesenko, J., Lander, A.D., and Calof, A.L. (2003). Widespread defects in the primary olfactory pathway caused by loss of *Mash1* function. J. Neurosci., in press.

Nakamura, T., Takio, K., Eto, Y., Shibai, H., Titani, K., and Sugino, H. (1990). Activin-binding protein from rat ovary is follistatin. Science *247*, 836–838.

Nakashima, M., Toyono, T., Akamine, A., and Joyner, A. (1999). Expression of growth/differentiation factor *11*, a new member of the BMP/TGFb superfamily during mouse embryogenesis. Mech. Dev. *80*, 185–189.

Newfeld, S.J., Wisotzky, R.G., and Kumar, S. (1999). Molecular evolu-

tion of a developmental pathway: phylogenetic analyses of transforming growth factor-beta family ligands, receptors and Smad signal transducers. Genetics *152*, 783–795.

Oh, S.P., and Li, E. (1997). The signaling pathway mediated by the type IIB activin receptor controls axial patterning and lateral asymmetry in the mouse. Genes Dev. *11*, 1812–1826.

Parent, J.M., Yu, T.W., Leibowitz, R.T., Geschwind, D.H., Sloviter, R.S., and Lowenstein, D.H. (1997). Dentate granule cell neurogenesis is increased by seizures and contributes to aberrant network reorganization in the adult rat hippocampus. J. Neurosci. *17*, 3727–3738.

Polyak, K., Lee, M.H., Erdjument-Bromage, H., Koff, A., Roberts, J.M., Tempst, P., and Massague, J. (1994). Cloning of p27Kip1, a cyclin-dependent kinase inhibitor and a potential mediator of extracellular antimitogenic signals. Cell *78*, 59–66.

Potten, C.S., and Loeffler, M. (1990). Stem cells: attributes, cycles, spirals, pitfalls and uncertainties. Lessons for and from the crypt. Development *110*, 1001–1020.

Roberts, V.J., and Barth, S.L. (1994). Expression of messenger ribonucleic acids encoding the inhibin/activin system during mid- and late-gestation rat embryogenesis. Endocrinology *134*, 914–923.

Scheufler, C., Sebald, W., and Hulsmeyer, M. (1999). Crystal structure of human bone morphogenetic protein-2 at 2.7 Å resolution. J. Mol. Biol. *287*, 103–115.

Schneyer, A.L., Rzucidlo, D.A., Sluss, P.M., and Crowley, W.F., Jr. (1994). Characterization of unique binding kinetics of follistatin and activin or inhibin in serum. Endocrinology *135*, 667–674.

Shou, J., Rim, P.C., and Calof, A.L. (1999). BMPs inhibit neurogenesis by a mechanism involving degradation of a transcription factor. Nat. Neurosci. *2*, 339–345.

Shou, J., Murray, R.C., Rim, P.C., and Calof, A.L. (2000). Opposing effects of bone morphogenetic proteins on neuron production and survival in the olfactory receptor neuron lineage. Development *127*, 5403–5413.

Sloviter, R.S., Dean, E., Sollas, A.L., and Goodman, J.H. (1996). Apoptosis and necrosis induced in different hippocampal neuron populations by repetitive perforant path stimulation in the rat. J. Comp. Neurol. *366*, 516–533.

Taylor, W.E., Bhasin, S., Artaza, J., Byhower, F., Azam, M., Willard, D.H., Jr., Kull, F.C., Jr., and Gonzalez-Cadavid, N. (2001). Myostatin inhibits cell proliferation and protein synthesis in C2C12 muscle cells. Am. J. Physiol. Endocrinol. Metab. *280*, E221–E228.

Thomas, M., Langley, B., Berry, C., Sharma, M., Kirk, S., Bass, J., and Kambadur, R. (2000). Myostatin, a negative regulator of muscle growth, functions by inhibiting myoblast proliferation. J. Biol. Chem. *275*, 40235–40243.

Williams, R.W. (2000). Mapping genes that modulate brain development: a quantitative genetic approach. In Mouse Brain Development, A.F. Goffinet, and P. Rakic, eds. (New York: Springer Verlag), pp. 21–49.